iScience

CellPress
OPEN ACCESS

Article

Detection of SARS-CoV-2 with RAPID: A prospective cohort study

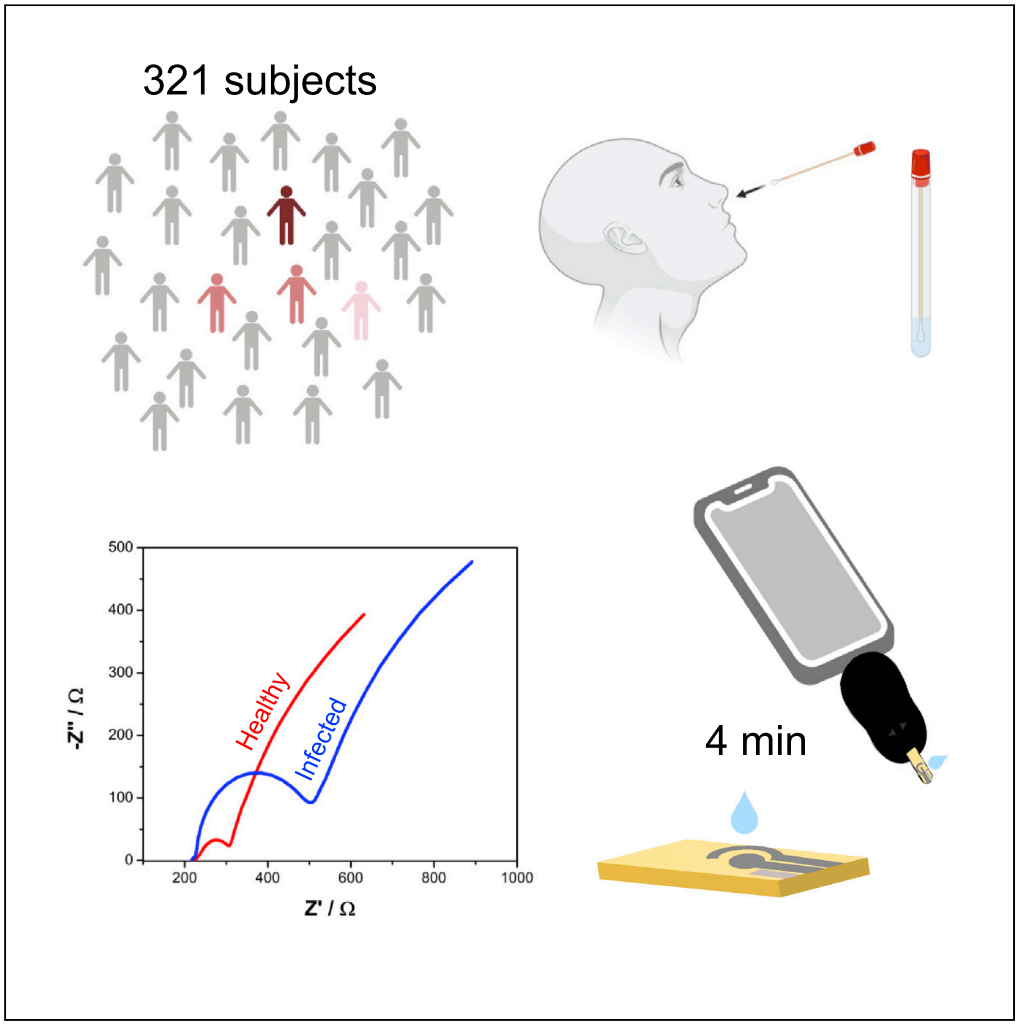

Marcelo D.T. Torres, Lucas F. de Lima, André L. Ferreira, ..., Antonio Dávila, Jr., Benjamin S. Abella, Cesar de la Fuente-Nunez

cfuente@upenn.edu

Highlights

RAPID shows high accuracy, sensitivity, and specificity in prospective cohort study

RAPID was successfully validated using 321 clinical samples

Effective point-of-care diagnosis of a heterogeneous sample set

Torres et al., iScience *25*, 104055
April 15, 2022
https://doi.org/10.1016/j.isci.2022.104055

iScience

CellPress
OPEN ACCESS

Article

Detection of SARS-CoV-2 with RAPID: A prospective cohort study

Marcelo D.T. Torres,[1,2,3] Lucas F. de Lima,[1,2,3,4] André L. Ferreira,[1,2,3,4] William R. de Araujo,[4] Paul Callahan,[5] Antonio Dávila, Jr.,[5] Benjamin S. Abella,[5] and Cesar de la Fuente-Nunez[1,2,3,6,*]

SUMMARY

COVID-19 has killed over 6 million people worldwide. Currently available methods to detect SARS-CoV-2 are limited by their cost and need for multistep sample preparation and trained personnel. Therefore, there is an urgent need to develop fast, inexpensive, and scalable point-of-care diagnostics that can be used for mass testing. Between January and March 2021, we obtained 321 anterior nare swab samples from individuals in Philadelphia (PA, USA). For the Real-time Accurate Portable Impedimetric Detection prototype 1.0 (RAPID) test, anterior nare samples were tested via an electrochemical impedance spectroscopy (EIS) approach. The overall sensitivity, specificity, and accuracy of RAPID in this cohort study were 80.6%, 89.0%, and 88.2%, respectively. We present a rapid, accurate, inexpensive (<$5.00 per unit), and scalable test for diagnosing COVID-19 at the point-of-care. We anticipate that further iterations of this approach will enable widespread deployment, large-scale testing, and population-level surveillance.

INTRODUCTION

COVID-19 has killed millions of people (World Health Organization, 2022) and continues to threaten healthcare systems worldwide. The widespread use of currently available diagnostics has been hampered by their high production cost, lack of scalability, and relatively slow detection times. Therefore, easy-to-use, low-cost, and rapid diagnostic tests are urgently needed.

Electrochemical impedance spectroscopy (EIS) is a technique traditionally used to characterize the surface of electrode materials and well suited to detect binding events between an agent and its recognition element functionalized onto a transducer surface (Bertok et al., 2019; Lisdat and Schäfer, 2008). Here, we describe the application of RAPID 1.0 (Real-time Accurate Portable Impedimetric Detection prototype 1.0) for simple, inexpensive, and rapid diagnosis of SARS-CoV-2 clinical samples (Figure 1).

RAPID is an electrochemical biosensor that measures changes in the resistance to charge transfer (R_{CT}) of the redox probe $[Fe(CN)_6]^{3-/4-}$, which is induced when the SARS-CoV-2 spike protein binds to an electrode previously functionalized with human angiotensin-converting enzyme-2 (ACE2) (Torres et al., 2021). By using EIS, the binding between the spike protein and ACE2 can be captured via the generation of an electrochemical signal. Compared to other techniques, RAPID (US$4.67) is around 7–10 times cheaper than RT-PCR and at least two times cheaper than RT-LAMP and other low-cost electrochemical techniques (Alafeef et al., 2020), and it is as inexpensive as high-throughput serological ELISA tests (La Marca et al., 2020). The detection time of the RAPID assay (4 min) is substantially faster than conventional techniques (*e.g.*, RT-PCR – 45 min) and as rapid as the fastest COVID detection methods reported to date (Broughton et al., 2020; Jiao et al., 2020; de Lima et al., 2021; Moitra et al., 2020; Rashed et al., 2021; Torrente-Rodríguez et al., 2020). To assess the clinical performance of this diagnostic platform, here, we performed an accuracy study aimed at detecting SARS-CoV-2 in anterior nare samples and compared the results obtained to those from RT-PCR, the gold standard test for COVID-19 diagnosis.

RESULTS

Cohort details

Clinical enrollment was performed over of 10 weeks between January and March 2021, following the period with the most COVID-19 cases in Philadelphia (from November to December 2020), where an average of

[1]Machine Biology Group, Departments of Psychiatry and Microbiology, Institute for Biomedical Informatics, Institute for Translational Medicine and Therapeutics, Perelman School of Medicine, University of Pennsylvania, Philadelphia, PA, USA

[2]Departments of Bioengineering and Chemical and Biomolecular Engineering, School of Engineering and Applied Science, University of Pennsylvania, Philadelphia, PA, USA

[3]Penn Institute for Computational Science, University of Pennsylvania, Philadelphia, PA, USA

[4]Portable Chemical Sensors Lab, Department of Analytical Chemistry, Institute of Chemistry, State University of Campinas - UNICAMP, Campinas, Sao Paulo, Brazil

[5]Penn Acute Research Collaboration, Department of Emergency Medicine, University of Pennsylvania, Philadelphia, PA, USA

[6]Lead contact

*Correspondence: cfuente@upenn.edu

https://doi.org/10.1016/j.isci.2022.104055

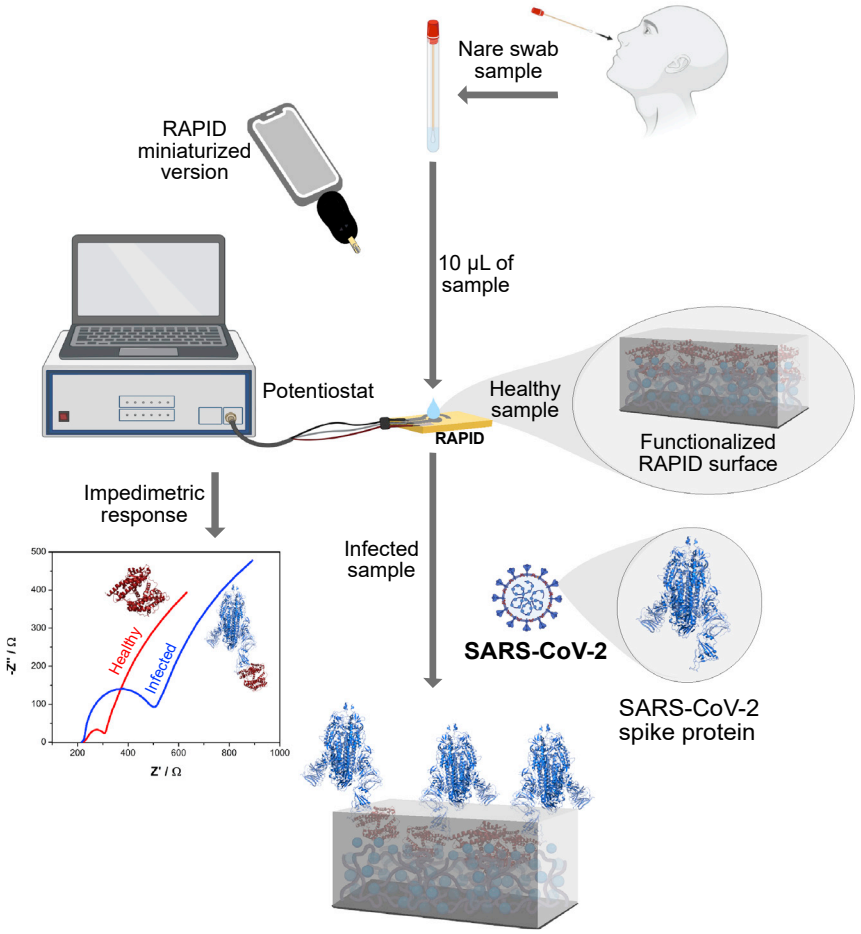

Figure 1. Detection of SARS-CoV-2 using RAPID in a prospective cohort study

RAPID diagnoses COVID-19 in nare swab samples infected with SARS-CoV-2. Ten microliters of the anterior nare sample were deposited on top of the biosensor functionalized with ACE2, which acts as the recognition agent for the viral spike protein. Impedimetric measurements were performed after 2 min of incubation time. Recognition of the SARS-CoV-2 spike protein by ACE2 led to an increased resistance signal measured by electrochemical impedance spectroscopy compared to the control group (*i.e.*, the medium where the collected sample was immersed). This figure was created with BioRender.com.

40,000 tests were performed with around 500 daily COVID-19 cases confirmed (prevalence of ~1.25% from November to December) (Figure 2A). All samples collected for the study were aliquoted and frozen at −80°C promptly after collection. The anterior nare samples were immersed in VTM following the Food and Drug Administration (FDA) recommendation for regulatory applications (Food and Drug Administration (FDA), 2021). We analyzed a total of 321 nare swab samples from incoming patients that agreed to donate their samples.

Analysis of the clinical samples

Clinical samples were incubated for 2 min onto the surface of the electrode, as this was determined to be the optimal amount of time needed to ensure viral detection using RAPID (Torres et al., 2021). The modified electrode favors rapid interaction kinetics between the SARS-CoV-2 spike protein and immobilized ACE2 (kinetics constant rate of 10^4 $M^{-1}s^{-1}$; Yang et al., 2020). RAPID's results are available within 4 min (2 min of sample incubation +2 min to perform the EIS analysis), which is faster than currently used methods for diagnosing COVID-19 (Bhalla et al., 2020). An additional 4 min were needed to run each blank; however, we did not consider this when calculating our testing time because the blanking step was performed prior to clinical sample analysis. Before starting our clinical study, we calibrated our biosensor using solutions of inactivated SARS-CoV-2 ranging from 10^1 to 10^6 PFU mL^{-1}. Complete clinical data paired with the

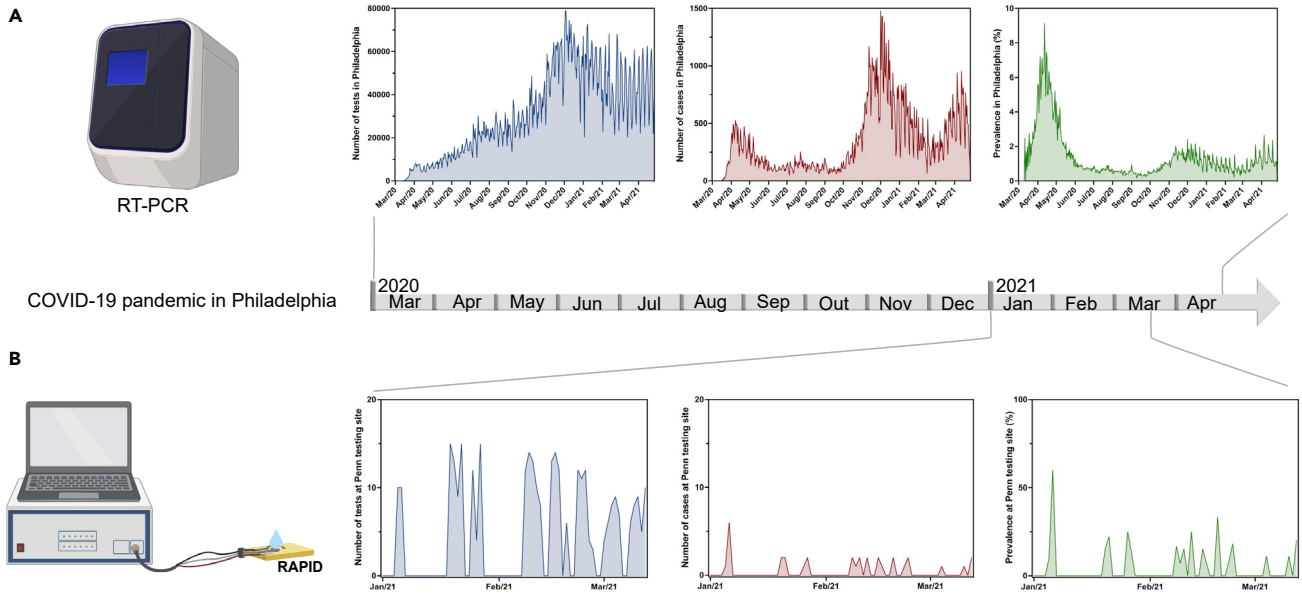

Figure 2. Clinical study in the context of the COVID-19 pandemic in Philadelphia

(A) Number of tests, number of cases, and prevalence of COVID-19 in Philadelphia as per official records (Centers for Disease Control and Prevention, 2021).

(B) Number of tests, number of cases, and prevalence in our retrospective cohort study. Part of this figure was created with BioRender.com.

gold-standard method RT-PCR were used to confirm the COVID-19 status of each of the 321 samples (Figure 2B). We obtained a total of 31 positive and 290 negative COVID-19 samples. RAPID demonstrated high sensitivity (80.7%), specificity (89.0%), and accuracy (88.2%) (Tables 1 and S1. Diagnosis of anterior nare samples using RAPID), when using a cut-off value of 0.100 for the normalized R_{CT}. The presence or absence of symptoms and other medical conditions did not interfere with the results obtained with RAPID, and no correlation was found between other medical conditions, race, gender, or age with the false positives and negative data obtained (Data S1. Patient demographic and clinical status). Compared to other electrochemical methods, molecular tests, colorimetric assays, and diagnostic tests reported in the literature (Table 2), RAPID presents one of the highest sensitivities reported to date (LOD of 2.8 fg mL^{-1} SARS-CoV-2 spike protein). In addition, RAPID displays a rapid detection time for SARS-CoV-2 (4 min) and is low cost (<US$5.00) compared to other diagnostic tests (Alafeef et al., 2020; Broughton et al., 2020; Jiao et al., 2020; Moitra et al., 2020; Qiu et al., 2020; Rashed et al., 2021; Torrente-Rodríguez et al., 2020; Yakoh et al., 2021; Zhao et al., 2021).

DISCUSSION

Currently, available diagnostic tests do not provide a sufficiently accurate, rapid, and affordable diagnosis of COVID-19. For instance, commercial SARS-CoV-2 antigen tests only detect virus concentrations characteristic of later stages of the disease at which patients are already highly infectious (Corman et al., 2021), thus not accurately controlling viral spread. RT-PCR, the gold standard for testing, presents optimal accuracy 3–5 days after the onset of symptoms (Boum et al., 2021). The affordability aspect is also particularly important if we are to ensure health equity and increased access to valuable tools, such as diagnostic tests, for preventing viral spread in disadvantaged communities and low-resource settings.

In this prospective cohort study, we assessed the performance of RAPID using 321 anterior nare swab samples from a diversified pool of subjects with ages ranging from 18 to 78 years old, different races, genders, COVID-19-related symptoms, and other medical conditions (Table 3). The clinical prevalence of positive COVID-19 cases in the set of samples analyzed was 9.7%, which is higher than the mean observed for the same period in Philadelphia (1%–2%; Figure 2). We did not find statistical correlations between the erroneously diagnosed samples by RAPID and the clinical status or any relevant information obtained from the participants (Table 3 and Data S1. Patient demographic and clinical status). False-positive results may be due to the use of angiotensin-converting enzyme inhibitors or angiotensin receptor blockers that may interact with RAPID's ACE2-modified electrode. However, the lack of information about the

Table 1. Clinical assessment of RAPID detection of SARS-CoV-2

	RT-qPCR						
RAPID	Positive (N = 31)	Negative (N = 290)	Total (N = 321)	Sensitivity	Specificity	Prevalence	Accuracy
Positive	25	32	57	25/31 (80.6%)		31/321 (9.7%)	283/321 (88.2%)
Negative	6	258	264		258/290 (89.0%)		

Positive and negative values obtained by RT-qPCR and sensitivity, specificity, and accuracy of RAPID 1.0 using nare samples

medication usage of participants limited our ability to draw such a correlation. Biofouling constitutes another important source of potential errors. Biofouling consists of non-specific interactions between the electrodic surface and proteins, lipids, and other biomolecules such as amino acids and glycoproteins that are part of complex clinical samples. These effects have been reported in the literature for complex biological samples (Jamal et al., 2020; Zou et al., 2020) and discussed in our previous work (Torres et al., 2021). Given that the goal of this study was to assess the suitability of the RAPID approach for point-of-care applications while obviating the need for sophisticated infrastructure or multistep analysis, we avoided performing any pretreatment of the samples and, instead, focused our efforts on enhancement of the robustness of the biosensor through the blocking of remaining active sites of the electrode with bovine serum albumin and the addition of a permselective Nafion layer to help prevent biofouling. However, some molecules may still cross the protective layer and adsorb onto the surface of the electrode, thus hindering electron transfer of the redox probe (potassium ferricyanide/ferrocyanide). This will cause higher resistivity, resulting in a similar effect to that observed when the viral spike protein interacts with the ACE2 immobilized on the surface of the electrode. An approach to help decrease the false-positive rate involves increasing the cut-off value of the method, which in turn decreases the specificity issues but also decreases RAPID's sensitivity. For example, if we change the cut-off value of RAPID to $(Z\text{-}Z_0)/Z_0 \geq 0.127$ instead of $(Z\text{-}Z_0)/Z_0 \geq 0.100$ to express a positive diagnosis, the specificity of the method is enhanced to 92.07% but its sensitivity is reduced to 74.2%. The false-negative results (6 out of 31 samples) obtained by RAPID can be related to the low viral loads (*i.e.*, lower than RAPID's limit of detection; 6.29 fg mL^{-1} spike protein) of some of the clinical samples. Sample collection during the cohort study, involving self-collection, may contribute to the false-negative rate obtained. RAPID is an inexpensive and portable alternative to existing COVID-19 tests, allowing for decentralized diagnosis at the point-of-care. The fast detection (4 min) enabled by our approach is significantly lower than commercially available tests (Kaushik et al., 2020; Rashed et al., 2021; Uhteg et al., 2020), and could potentially be lowered further by using alternative recognition agents, such as engineered versions of human ACE2 with enhanced selective binding toward SARS-CoV-2, or engineered receptors (*e.g.*, antibodies) to the SARS-CoV-2 spike protein (Chan et al., 2020).

Finally, RAPID is amenable to multiplexing to allow detection of emerging biological threats such as bacteria, fungi, and other viruses, simply by adding other recognition agents and modifying the disposition of the electrodes (array configuration). Its ability to detect minimal viral particles within a sample allows diagnosing COVID-19 at the onset of the infection. Collectively, its low-cost, rapid detection time, and high analytical sensitivity make RAPID an exciting alternative tool for high-frequency COVID-19 testing and effective population surveillance (Mina et al., 2020).

Limitations of the study

The major limitation of this study is the shelf life of the biosensor due to ACE2 denaturation after several days anchored to the surface of the working electrode. Future work will focus on designing ACE2 derivatives possessing an extended shelf life.

STAR★METHODS

Detailed methods are provided in the online version of this paper and include the following:

- KEY RESOURCES TABLE
- RESOURCE AVAILABILITY
  - Lead contact
  - Materials availability
  - Data and code availability

Table 2. Side-by-side comparison of the analytical features between RAPID and different sensors developed for SARS-CoV-2 detection

Sensor	LOD	Target	Technique	Time (min)	Reference
RAPID	2.8 fg mL^{-1}	SARS-CoV-2 spike protein	EIS	4	(Torres et al., 2021)
LEAD	2.29 fg mL^{-1}	SARS-CoV-2 spike protein	SWV	6.5	(de Lima et al., 2021)
SARS-CoV-2 RapidFlex	500 pg mL^{-1}	Viral antigen nucleocapsid protein	DPV and OCP-EIS	10	(Torrente-Rodríguez et al., 2020)
	0.1 mg mL^{-1}	SARS-CoV-2 spike protein	EIS	3	(Rashed et al., 2021)
	1 μg mL^{-1}	IgM and IgG antibodies	SWV	3	(Yakoh et al., 2021)
DETECTR	10 RNA copies μL^{-1}	*E* gene and *N* gene	CRISPR technology	40	(Broughton et al., 2020)
COLOR	154 fg mL^{-1}	SARS-CoV-2 spike protein	Colorimetric	5	(Ferreira et al., 2021)
SARS-CoV-2@f-AuNPs	Ct value: 36.5	Antibody (S, E, and M)	Colorimetric	3	(Ventura et al., 2020)
Lateral flow immunoassay (LFIA)	ND	COVID-19 IgG and IgM antibody	Colorimetric	15	5
DNAzyme and SARS-CoV-2 RNA	0.01 ng mL^{-1}	SARS-CoV-2 RNA	Colorimetric	±5	(Anantharaj et al., 2020)
RT-LAMP	0.75 RNA copies μL^{-1}	SARS-CoV-2 RNA	Colorimetric	15–40	(Yu et al., 2020)
LAMP	50 RNA copies μL^{-1}	SARS-CoV-2 RNA	Fluorescence	>40	(Ganguli et al., 2020)
Lateral flow immunoassay (LFIA)	0.65 ng mL^{-1}	Biotinylated antibody	Colorimetric	ND	(Grant et al., 2020)
Lateral flow immunoassay (LFIA)	1 pg mL^{-1}	Protein-anti-SARS-CoV-2 IgM/IgG	Colorimetric	25	(Liu et al., 2021)
Lateral flow immunoassay (LFIA)	(IgG) 0.121 U L^{-1} and (IgM) 0.366 U L^{-1}	Antibody IgG and IgM	Fluorescent	15	(Zhang et al., 2020)

Antibody (S, E, and M) spike, envelope, and membrane; gold nanoparticles (AuNP), functionalized AuNanos (f-AuNPs), ribonucleic acid (RNA); transcription loop-mediated isothermal amplification (RT-LAMP); Electrochemical impedance spectroscopy (EIS); Differential pulse voltammetry (DPV); Open-circuit potential-electrochemical impedance spectroscopy (OCP-EIS); Square-wave voltammetry (SWV); Reverse transcription loop-mediated isothermal amplification (RT-LAMP); ND (not described).

SUPPLEMENTAL INFORMATION

Supplemental information can be found online at https://doi.org/10.1016/j.isci.2022.104055.

ACKNOWLEDGMENTS

C.F.-N. holds a Presidential Professorship at the University of Pennsylvania, is a recipient of the Langer Prize by the AIChE Foundation and acknowledges funding from the Institute for Diabetes, Obesity, and Metabolism, the Penn Mental Health AIDS Research Center of the University of Pennsylvania, the National Institute of General Medical Sciences of the National Institutes of Health under award number R35GM138201, and the Defense Threat Reduction Agency (DTRA; HDTRA11810041 and HDTRA1-21-1-0014). Research reported in this publication was supported by the Nemirovsky Prize and by funds provided by the Dean's

Table 3. Demographic information of the subjects tested

	Total Cohort (n = 321)	Positive Subjects (n = 31)	Negative Subjects (n = 290)
Median age	37 (13)	36 (14)	37 (13)
Gender			
Male	91 (28%)	9 (29%)	82 (28%)
Female	230 (72%)	22 (71%)	208 (72%)
Race			
Caucasian	133 (41%)	13 (42%)	120 (41%)
African American	147 (46%)	16 (52%)	131 (45%)
Hispanic	13 (4%)	2 (6%)	11 (4%)
Other	29 (9%)	0	29 (10%)
Medical Problems			
Asthma	66 (21%)	7 (23%)	59 (20%)
Hypertension	61 (19%)	8 (26%)	53 (18%)
History of Smoking	41 (13%)	3 (10%)	38 (13%)
Diabetes	28 (9%)	5 (16%)	23 (8%)
No Medical History	176 (55%)	16 (52%)	160 (55%)
Symptoms			
Cough	93 (29%)	14 (45%)	79 (27%)
Headache	68 (21%)	11 (35%)	57 (20%)
Fever/Chills	67 (21%)	11 (35%)	56 (19%)
Shortness of Breath	33 (10%)	3 (10%)	30 (10%)
No Symptoms	127 (40%)	6 (19%)	121 (42%)

Innovation Fund from the Perelman School of Medicine at the University of Pennsylvania. B.S.A. acknowledges funds provided by the Dean's Innovation Fund from the Perelman School of Medicine at the University of Pennsylvania. We thank Jonathan A. Epstein for his support. This work was approved by the University of Pennsylvania Institutional Review Board (IRB 844145). All figures were created with BioRender.com.

AUTHOR CONTRIBUTIONS

Conceptualization, M.D.T.T., W.R.A., and C.F.-N.; Methodology, M.D.T.T., L.F.L., A.L.F., W.R.A., P.C., and A.D.; Writing – Reviewing & Editing, M.D.T.T., W.R.A., A.D., B.S.A., and C.F.-N.; Supervision, B.S.A. and C.F.-N.; Data Curation, M.D.T.T., L.F.L., A.L.F., W.R.A., P.C., and A.D.

DECLARATION OF INTERESTS

A non-provisional patent application has been filed on related work.

Received: August 4, 2021
Revised: January 20, 2022
Accepted: March 7, 2022
Published: April 15, 2022

REFERENCES

Alafeef, M., Dighe, K., Moitra, P., and Pan, D. (2020). Rapid, ultrasensitive, and quantitative detection of SARS-CoV-2 using antisense oligonucleotides directed electrochemical biosensor chip. ACS Nano *14*, 17028–17045.

Anantharaj, A., Das, S.J., Sharanabasava, P., Lodha, R., Kabra, S.K., Sharma, T.K., and Medigeshi, G.R. (2020). Visual detection of SARS-CoV-2 RNA by conventional PCR-induced generation of DNAzyme sensor. Front. Mol. Biosci. *7*, 1–7.

Bertok, T., Lorencova, L., Chocholova, E., Jane, E., Vikartovska, A., Kasak, P., and Tkac, J. (2019). Electrochemical impedance spectroscopy based biosensors: mechanistic principles, analytical examples and challenges towards commercialization for assays of protein cancer biomarkers. ChemElectroChem *6*, 989–1003.

Bhalla, N., Pan, Y., Yang, Z., and Payam, A.F. (2020). Opportunities and challenges for biosensors and nanoscale Analytical tools for pandemics: COVID-19. ACS Nano *14*, 7783–7807.

Boum, Y., Fai, K.N., Nicolay, B., Mboringong, A.B., Bebell, L.M., Ndifon, M., Abbah, A., Essaka, R., Eteki, L., Luquero, F., et al. (2021). Performance and operational feasibility of antigen and antibody rapid diagnostic tests for COVID-19 in symptomatic and asymptomatic patients in Cameroon: a clinical, prospective, diagnostic accuracy study. Lancet Infect. Dis. *21*, 1089–1096.

Broughton, J.P., Deng, X., Yu, G., Fasching, C.L., Servellita, V., Singh, J., Miao, X., Streithorst, J.A., Granados, A., Sotomayor-Gonzalez, A., et al. (2020). CRISPR–Cas12-based detection of SARS-CoV-2. Nat. Biotechnol. *38*, 870–874.

Centers for Disease Control and Prevention. (2022). COVID Data Tracker. US Department of Health and Human Services, CDC, Atlanta, GA. https://covid.cdc.gov/covid-data-tracker/#datatracker-home.

Chan, K.K., Dorosky, D., Sharma, P., Abbasi, S.A., Dye, J.M., Kranz, D.M., Herbert, A.S., and Procko, E. (2020). Engineering human ACE2 to optimize binding to the spike protein of SARS coronavirus 2. Science. *369*, 1261–1265.

Corman, V.M., Haage, V.C., Bleicker, T., Schmidt, M.L., Mühlemann, B., Zuchowski, M., Jo, W.K., Tscheak, P., Möncke-Buchner, E., Müller, M.A., et al. (2021). Comparison of seven commercial SARS-CoV-2 rapid point-of-care antigen tests: a single-centre laboratory evaluation study. Lancet Microbe *2*, e311–e319.

de Lima, L.F., Ferreira, A.L., Torres, M.D.T., de Araujo, W.R., and de la Fuente-Nunez, C. (2021). Minute-scale detection of SARS-CoV-2 using a low-cost biosensor composed of pencil graphite electrodes. Proc. Natl. Acad. Sci. U S A *118*, e2106724118.

e Silva, R.F., Longo Cesar Paixão, T.R., Der Torossian Torres, M., and de Araujo, W.R. (2020). Simple and inexpensive electrochemical paper-based analytical device for sensitive detection of Pseudomonas aeruginosa. Sensor. Actuator. B Chem. *308*, 127669.

Ferreira, A.L., de Lima, L.F., Torres, M.D.T., de Araujo, W.R., and de la Fuente-Nunez, C. (2021). Low-cost optodiagnostic for minute-time scale detection of SARS-CoV-2. ACS Nano *15*, 17453–17462.

Food and Drug Administration (FDA) (2021). Emergency Use Authorization (EUA) Summary iC SARS-CoV-2 Test, https://www.fda.gov/media/142596/download#:~:text=The%20iC%20SARS%2DCoV2%20Test,Drug%20Administration's%20Emergency%20Use%20Authorization.

Ganguli, A., Mostafa, A., Berger, J., Aydin, M.Y., Sun, F., Stewart de Ramirez, S.A., Valera, E., Cunningham, B.T., King, W.P., and Bashir, R. (2020). Rapid isothermal amplification and portable detection system for SARS-CoV-2. Proc. Natl. Acad. Sci. U S A *117*, 22727–22735.

Grant, B.D., Anderson, C.E., Williford, J.R., Alonzo, L.F., Glukhova, V.A., Boyle, D.S., Weigl, B.H., and Nichols, K.P. (2020). SARS-CoV-2 coronavirus nucleocapsid antigen-detecting half-strip lateral flow assay toward the development of point of care tests using commercially available reagents. Anal. Chem. *92*, 11305–11309.

Jamal, A.J., Mozafarihashjin, M., Coomes, E., Powis, J., Li, A.X., Paterson, A., Anceva-Sami, S., Barati, S., Crowl, G., Faheem, A., et al. (2020). Sensitivity of nasopharyngeal swabs and saliva for the detection of severe acute respiratory syndrome coronavirus 2. Clin. Infect. Dis. *72*, 1064–1066.

Jiao, J., Duan, C., Xue, L., Liu, Y., Sun, W., and Xiang, Y. (2020). DNA nanoscaffold-based SARS-CoV-2 detection for COVID-19 diagnosis. Biosens. Bioelectron. *167*, 112479.

Kaushik, A.K., Dhau, J.S., Gohel, H., Mishra, Y.K., Kateb, B., Kim, N.-Y., and Goswami, D.Y. (2020). Electrochemical SARS-CoV-2 sensing at point-of-care and artificial intelligence for intelligent COVID-19 management. ACS Appl. Bio Mater. *3*, 7306–7325.

La Marca, A., Capuzzo, M., Paglia, T., Roli, L., Trenti, T., and Nelson, S.M. (2020). Testing for SARS-CoV-2 (COVID-19): a systematic review and clinical guide to molecular and serological in-vitro diagnostic assays. Reprod. Biomed. Online *41*, 483–499.

Lisdat, F., and Schäfer, D. (2008). The use of electrochemical impedance spectroscopy for biosensing. Anal. Bioanal. Chem. *391*, 1555–1567.

Liu, H., Dai, E., Xiao, R., Zhou, Z., Zhang, M., Bai, Z., Shao, Y., Qi, K., Tu, J., Wang, C., et al. (2021). Development of a SERS-based lateral flow immunoassay for rapid and ultra-sensitive detection of anti-SARS-CoV-2 IgM/IgG in clinical samples. Sensor. Actuator. B Chem. *329*, 129196.

Mauritz, K.A., and Moore, R.B. (2004). State of understanding of nafion. Chem. Rev. *104*, 4535–4586.

Mina, M.J., Parker, R., and Larremore, D.B. (2020). Rethinking covid-19 test sensitivity — a strategy for containment. N. Engl. J. Med. *383*, e120.

Moitra, P., Alafeef, M., Dighe, K., Frieman, M.B., and Pan, D. (2020). Selective naked-eye detection of SARS-CoV-2 mediated by N gene targeted antisense oligonucleotide capped plasmonic nanoparticles. ACS Nano *14*, 7617–7627.

Muñoz, J., Montes, R., and Baeza, M. (2017). Trends in electrochemical impedance spectroscopy involving nanocomposite transducers: characterization, architecture surface and bio-sensing. TrAC Trends Anal. Chem. *97*, 201–215.

Qiu, G., Gai, Z., Tao, Y., Schmitt, J., Kullak-Ublick, G.A., and Wang, J. (2020). Dual-functional plasmonic photothermal biosensors for highly accurate severe acute respiratory syndrome coronavirus 2 detection. ACS Nano *14*, 5268–5277.

Rashed, M.Z., Kopechek, J.A., Priddy, M.C., Hamorsky, K.T., Palmer, K.E., Mittal, N., Valdez, J., Flynn, J., and Williams, S.J. (2021). Rapid detection of SARS-CoV-2 antibodies using electrochemical impedance-based detector. Biosens. Bioelectron. *171*, 112709.

Torrente-Rodríguez, R.M., Lukas, H., Tu, J., Min, J., Yang, Y., Xu, C., Rossiter, H.B., and Gao, W. (2020). SARS-CoV-2 RapidPlex: a graphene-based multiplexed telemedicine platform for rapid and low-cost COVID-19 diagnosis and monitoring. Matter *3*, 1981–1998.

Torres, M.D.T., de Araujo, W.R., de Lima, L.F., Ferreira, A.L., and de la Fuente-Nunez, C. (2021). Low-cost biosensor for rapid detection of SARS-CoV-2 at the point of care. Matter *4*, 2403–2416.

Uhteg, K., Jarrett, J., Richards, M., Howard, C., Morehead, E., Geahr, M., Gluck, L., Hanlon, A., Ellis, B., Kaur, H., et al. (2020). Comparing the analytical performance of three SARS-CoV-2 molecular diagnostic assays. J. Clin. Virol. *127*, 104384.

Uygun, Z.O., and Ertuğrul Uygun, H.D. (2014). A short footnote: circuit design for faradaic impedimetric sensors and biosensors. Sensor. Actuator. B Chem. *202*, 448–453.

Ventura, B.D., Cennamo, M., Minopoli, A., Campanile, R., Censi, S.B., Terracciano, D., Portella, G., and Velotta, R. (2020). Colorimetric test for fast detection of SARS-COV-2 in nasal and throat swabs. ACS Sens. *5*, 3043–3048.

World Health Organization (2022). WHO Coronavirus (COVID-19) Dashboard.

Yakoh, A., Pimpitak, U., Rengpipat, S., Hirankarn, N., Chailapakul, O., and Chaiyo, S. (2021). Paper-based electrochemical biosensor for diagnosing COVID-19: detection of SARS-CoV-2 antibodies and antigen. Biosens. Bioelectron. *176*, 112912.

Yang, J., Petitjean, S.J.L., Koehler, M., Zhang, Q., Dumitru, A.C., Chen, W., Derclaye, S., Vincent, S.P., Soumillion, P., and Alsteens, D. (2020). Molecular interaction and inhibition of SARS-CoV-2 binding to the ACE2 receptor. Nat. Commun. *11*, 4541.

Yu, L., Wu, S., Hao, X., Dong, X., Mao, L., Pelechano, V., Chen, W.-H., and Yin, X. (2020). Rapid Detection of COVID-19 Coronavirus Using a Reverse Transcriptional Loop-Mediated Isothermal Amplification (RT-LAMP) Diagnostic Platform. Clin. Chem. *66*, 975–977. https://doi.org/10.1093/clinchem/hvaa102.

Zhang, C., Zhou, L., Liu, H., Zhang, S., Tian, Y., Huo, J., Li, F., Zhang, Y., Wei, B., Xu, D., et al. (2020). Establishing a high sensitivity detection method for SARS-CoV-2 IgM/IgG and developing a clinical application of this method. Emerg. Microb. Infect. *9*, 2020–2029.

Zhao, H., Liu, F., Xie, W., Zhou, T.-C., OuYang, J., Jin, L., Li, H., Zhao, C.-Y., Zhang, L., Wei, J., et al. (2021). Ultrasensitive supersandwich-type electrochemical sensor for SARS-CoV-2 from the infected COVID-19 patients using a smartphone. Sensor. Actuator. B Chem. *327*, 128899.

Zou, L., Ruan, F., Huang, M., Liang, L., Huang, H., Hong, Z., Yu, J., Kang, M., Song, Y., Xia, J., et al. (2020). SARS-CoV-2 viral load in upper respiratory specimens of infected patients. N. Engl. J. Med. *382*, 1177–1179.

STAR★METHODS

KEY RESOURCES TABLE

REAGENT or RESOURCE	SOURCE	IDENTIFIER
Chemicals, peptides, and recombinant proteins		
Human angiotensin converting enzyme 2 (ACE2)	GenScript	Z03484-1
Sulfuric acid (H_2SO_4)	Sigma	258105-1L-PC
Potassium chloride (KCl)	Sigma	P3911-1KG
Potassium ferricyanide $K_3[Fe(CN)_6]$	Sigma	244023-5G
Potassium ferrocyanide $K_4[Fe(CN)_6]$	Sigma	P3289-5G
Bovine serum albumine (BSA)	Sigma	A2153-10G
Glutaraldehyde (GA)	Fisher	S25341
Nafion	Sigma	527084-25ML
Phosphate saline buffer (PBS)	VWR	P32200
Software and Algorithms		
Squidstat	Admiral Instruments	
MultiAutolab M101	Metrohm	

RESOURCE AVAILABILITY

Lead contact

Further information and requests for resources should be directed to and will be fulfilled by the Lead Contact, Dr. Cesar de la Fuente-Nunez (cfuente@upenn.edu).

Materials availability

This study did not generate new unique reagents.

Data and code availability

Data: The diagnostics results used for analysis and the detailed demographic table are available at Mendeley data (https://doi.org/10.17632/y7f78c8627.1).

Code: This work did not generate any code.

Any additional information required to reanalyze the data reported in this paper is available from the lead contact upon request.

EXPERIMENTAL MODEL AND SUBJECT DETAILS

Anterior nare sample collection and processing

The collection of the anterior nare samples was performed by the subjects tested under supervision by clinical research staff at the Penn Presbyterian Medical Center (PPMC). All the demographic information, as well as the presence or absence of symptoms of the individuals tested, are shown in Table 1. The samples were stabilized and stored in viral transport medium (VTM) following CDC guidelines (CDC SOP#: DSR-052-05). The anterior nare samples were maintained on ice during the collection period, separated into identical aliquots and subsequently stored at −80°C and readily tested. Care was taken to ensure samples were thawed only once before testing.

METHOD DETAILS

RAPID biosensor preparation

The testing platform comprises two components: the electrochemical sensor and a potentiostat. The electrochemical sensors were prepared following established protocols (Torres et al., 2021). Briefly, the

portable devices were printed in a three-electrode configuration cell on phenolic circuit board material (2 × 2 cm). Electrically conductive carbon and Ag/AgCl inks were used for the screen-printing process to fabricate the working/auxiliary electrodes and reference electrodes, respectively. The working electrode's carbon surface was modified using the drop-casting method. First, 4 μL of 25% glutaraldehyde (GA) solution was added for 1 hour at 37°C to allow the formation of a cross-linked polymer, which enabled subsequent anchoring of ACE2 (4 μL at 0.32 mg mL^{-1}). ACE2 was then incubated at 37°C for 1.5 hours. Next, we added 4 μL of bovine serum albumin (BSA) at 1 mg mL^{-1} and allowed the working electrode (WE) to dry for 0.5 hours at 37°C to stabilize the enzyme and block potential active sites present within the modified carbon electrode, to avoid nonspecific adsorption of other proteins to the glutaraldehyde layer and ensure stabilization of the ACE2 tertiary structure. Since our goal was to simplify the detection of SARS-CoV-2 in complex biological samples, such as anterior nare swabs, we added a 1 wt. % Nafion solution as an additional protective layer. Nafion, an anionic and selective membrane that allows the permeation of cationic species, is commonly used to enhance the sensitivity and robustness of electrochemical sensors(Mauritz and Moore, 2004). The membrane formed by 1 wt. % Nafion solution enhanced the sensitivity of RAPID 1.0, by enabling chemical preconcentration of cation species and protecting the electrode's surface against biofouling by macromolecules present in biological samples, such as proteins and lipids(e Silva et al., 2020).

RAPID test for SARS-CoV-2 diagnosis

SquidStat Plus (Admiral Instruments, software Squidstat) and MultiAutolab M101 (Metrohm, NOVA 2.1) potentiostats were used to record all data. The electrodes were characterized by Cyclic Voltammetry (CV) and EIS techniques using a mixture of 5 mmol L^{-1} potassium ferricyanide/ferrocyanide in 0.1 mol L^{-1} KCl solution before and after electrode modification with glutaraldehyde, ACE2, BSA, and Nafion. CVs and EIS were recorded using a potential ranging from 0.7 to −0.3 V at the scan rate of 50 mV s^{-1} and a frequency ranging from 10^5 to 10^{-1} Hz using a sinusoidal signal with 10 mV of amplitude at room temperature, respectively.

Here, we explored the selective binding between ACE2, which was immobilized on the electrode surface, and SARS-CoV-2 spike protein. The receptor ACE2 is the known entry point for the virus in humans, the SARS-CoV-2 spike protein is its binding element (Yang et al., 2020). The interaction between these two molecules leads to lower interfacial electron transfer rates between the redox probe, ferricyanide/ferrocyanide, and the electrode surfaces. To track this change, we monitored the charge-transfer resistance (R_{CT}), *i.e.*, the diameter of the semi-arc on the Nyquist plot, which correlates with the number of spike protein molecules bound to the electrode's surface (Muñoz et al., 2017). The EIS measurements were performed using 200 μL of a mixture of 5 mmol L^{-1} ferricyanide/ferrocyanide prepared in a 0.1 mol L^{-1} KCl solution added after incubating the clinical sample (10 μL of anterior nare sample) for 2 minutes on the electrode surface. A gentle washing step using PBS was performed to remove the sample and any unbound SARS-CoV-2. For the EIS measurement, a sinusoidal signal was applied at room temperature in the frequency range between 10^5 and 10^{-1} s^{-1} using a typical open circuit potential of 0.15 V and an amplitude of 10 mV.

RT-PCR analysis

For the RT-PCR assays, RNA was extracted and purified using the QIAmp DSP Viral RNA Mini Kit (Qiagen) from a 140 μL aliquot immediately after the samples were collected and all the positive samples were re-analyzed after the cohort study was over. The first step of this process chemically inactivated the virus from the anterior nare samples under highly denaturing conditions (guanidine thiocyanate) and was performed in a biosafety cabinet under BSL-2 enhanced protocols. The remainder of the process was performed at the lab bench under standard conditions using the vacuum protocol as per manufacturer's instructions. The elution and input volumes used were 140 μL. Next, RNA present in the samples was analyzed in duplicate using the TaqPath™ 1-Step RT-qPCR reagent (Life Technologies) on the Quantstudio 7 Flex Genetic Analyzer (ABI). The oligonucleotide primers and probes for detection of 2019-nCoV were selected from regions of the virus nucleocapsid (N) gene. The panel was designed for specific detection of the 2019-nCoV viral RNA (two primer/probe sets, N1 and N2). An additional primer/probe set to detect the human RNase P gene (RP) in control samples and clinical specimens was also included in the panel (2019-nCoVEUA-01). RNaseP is a single copy human-specific gene and can indicate the number of human cells collected. Table S2. RT-PCR panel primers and probes, lists the CDC-recommended 2019-nCoV RT-PCR primers and probes used for all the experiments.

Prospective cohort study design and participants

The performance of RAPID was assessed using both SARS-CoV-2-positive and negative samples from an ambulatory COVID-19 testing site for the public, led by staff at the Penn Presbyterian Medical Center (PPMC). All participants underwent anterior nare testing for SARS-CoV-2 using CLIA-approved RT-PCR by PPMC staff for testing, and after this testing underwent study procedures. Adult (age > 17 years) subjects were eligible if they (1) underwent PPMC staff-led testing immediately prior to study enrollment, (2) were deemed competent for written consent, (3) were English fluent, and (4) did not have any contraindications to anterior nare samples collection procedures, such as recent facial surgery or active head and neck cancer. Subjects completed standard written consent, and then completed a short survey including demographic information and recent infectious symptoms, if any. Subjects then underwent anterior nasal swabbing supervised by trained clinical research coordinators. This work was approved by the University of Pennsylvania Institutional Review Board (IRB 844145).

Diagnosis and statistical analysis

The R_{CT} values of Nyquist plots obtained using Squidstat Plus (Admiral Instruments) and Multi Autolab M101 (Metrohm) were extracted by the application of an equivalent circuit using the softwares Zahner Analysis and Nova 2.1, respectively. We created an equivalent circuit comprising two semi-arc regions obtained during the electrochemical experiments in the Nyquist plots. The first region is a non-defined semi-arc at a high-frequency range, which is caused by inhomogeneity or defects in the electrode modification step (during drop-casting functionalization) and considerably small (R_{CT} ~10 Ω) (Bertok et al., 2019; Uygun and Ertuğrul Uygun, 2014). The second parallel component of the equivalent circuit comprises an R_{CT}, whose signal intensity was proportional to the logarithm of the concentration of SARS-CoV-2, and presented a Warburg element to describe the mass transport (diffusional control).

To diagnose a given sample, we used the normalized R_{CT}, defined by the following equation:

$$\text{normalized } R_{CT} = \frac{Z - Z_0}{Z_0}$$

where Z is the R_{CT} of the sample and Z_0 is the R_{CT} of the blank solution (VTM).

We set as a cut-off value a 10% change in the R_{CT} when compared to the blank solution, *i.e.*, $(Z\text{-}Z0)/Z_0 \geq 0.100$ to diagnose as a positive result. Such a cut-off threshold considers the limit of quantification (LOQ) value previously obtained for inactivated virus 3.87 PFU mL^{-1} (Torres et al., 2021), thus allowing discrimination between SARS-CoV-2 negative and SARS-CoV-2 positive samples.

QUANTIFICATION AND STATISTICAL ANALYSIS

Normalized R_{CT} values extracted from EIS measurements are presented as an average of 3 different replicates for each sample. Graphs were created and statistical tests conducted in GraphPad Prism 9.2.